

# Effect of Blood Flow on Brain Temperature Distribution

M. Zhu<sup>1,2</sup>, J. J. Ackerman<sup>1,2</sup>, A. L. Sukstanskii<sup>2</sup>, D. A. Yablonskiy<sup>2,3</sup>

<sup>1</sup>Department of Chemistry, Washington University, Saint Louis, MO, United States, <sup>2</sup>Mallinckrodt Institute of Radiology, Washington University School of Medicine, Saint Louis, MO, United States, <sup>3</sup>Department of Physics, Washington University, Saint Louis, MO, United States

**Introduction** Direct measurements of temperature distribution in the rat brain reveal a temperature gradient with the center of the brain being warmer than the brain surface [1]. Detail theoretical analysis [2] predicts that the temperature distribution near the brain surface is exponential in behavior with a defining characteristic “screening” length  $\Delta$  dependent upon the cerebral blood flow (CBF). In this study, we provide direct experimental evidence confirming the theoretical relationship between the characteristic screening length and CBF. Consequently, it follows that measurement of brain temperature profile provides quantitative assessment of blood flow. Temperature profiles were determined by means of non-invasive MR spectroscopy and verified by direct thermocouple measurements. CBF was measured using the microsphere tracer technique.

**Methods** Male Sprague-Dawley rats weighting 260-400g were divided into three groups:

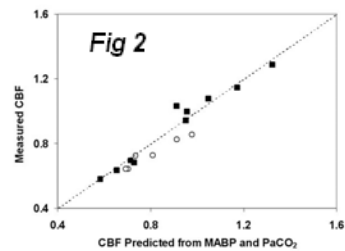
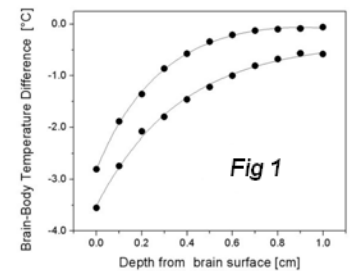
**Group 1 (Direct brain temperature measurement by thermocouple, n=10):** Rats under ketamine/xylazine anesthesia were catheterized for left femoral artery blood pressure and blood sampling. Rats were then intubated and mechanically ventilated with 30% O<sub>2</sub> balanced with 70% N<sub>2</sub>. Their torsos were maintained at 37°C with circulating water. Body temperature was monitored by thermocouple inserted 7 cm deep through the rectum. After 20 min, 1.2% isoflurane was introduced into the breathing gas. A 0.3 mm diameter burr-hole 2-3 mm anterior to and lateral from the lambda was drilled through the skull and a 36-gauge T-type thermocouple probe was fixed to the stereotaxic headframe. The temperature probe was then moved vertically downward from brain surface to the core of brain in 1 mm steps until it reached 10 mm deep. Temperature data from brain and rectum were recorded at the rate of 0.5 s<sup>-1</sup>.

**Group 2 (Absolute CBF measurement by microspheres, n=6):** After rats had been anesthetized and ventilated as described above, the left ventricle was catheterized through the right carotid artery until passing the ventricle valve. The left femoral artery was catheterized for arterial blood gases measurement and collecting reference blood for CBF calculation. Once blood gas parameters stabilized, a rapid 0.8 ml bolus of a well-mixed solution of microspheres (Samarium labeled, 15  $\mu$ m diameter) was injected into the left ventricle. Immediately prior to the microsphere injection, the syringe pump was switched on to collect femoral arterial blood at a rate of 0.5 ml/min for 2 min. Brain tissues of interest were sampled and sent for microsphere counting analysis together with dried reference blood.

**Group 3 (MR spectroscopy measurement of brain temperature, n=3):** Imaging and spectroscopy studies were performed on a Magnex 11.74T horizontal-bore magnet with an 8cm inner-diameter Magnex gradient insert controlled by a Varian INOVA console. Each rat was anesthetized and secured on a house-made Teflon® head holder as previously described [3]. Anesthesia was maintained with 1.2% isoflurane (in 100% O<sub>2</sub>) during the experimental session. Body temperature was monitored with fiber optical probe and recorded at a 0.2 s<sup>-1</sup> sampling rate. A transmit/receive single turn surface coil (i.d. 2.7cm) was secured on the top of rat head. A Localization Adiabatic Selective Refocusing (LASER) [4] sequence was used to collect single voxel MRS data with the following parameters: 4kHz bandwidth, TR=1.64s, TE=70ms, 512ms acquisition time, 2x2x2 mm<sup>3</sup> voxel size, and 600 averages. A vertical array of six such voxels was selected to profile brain temperature in a 1mm step from surface to the deep brain (Fig.3). Shimming was optimized for a region covering all the above voxels using FASTMAP [5]. Acquired FID signals were processed such that the N-Acetyl Aspartate (NAA) peak was set to zero and the water frequency was determined using single peak modeling by Varian’s Bayesian MRS spectrum analysis package.

**Results and Discussion** Two representative data sets from Group 1 rats showing difference between brain and body temperature ( $T_{\text{brain}} - T_{\text{body}}$ ) vs. brain depth are presented in Fig.1. Filled circles are experimental data; solid lines are curves representing the theoretical model (for details, see [2]). Difference between the curves reflects different physiological conditions as demonstrated by measurements of blood parameters (see below). Fitting of the theoretical equation to experimental data allows calculation of the CBF value from each rat under different physiological condition (characteristic length  $\Delta$  is inversely proportional to the square root of CBF).

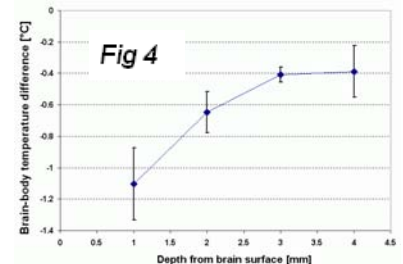
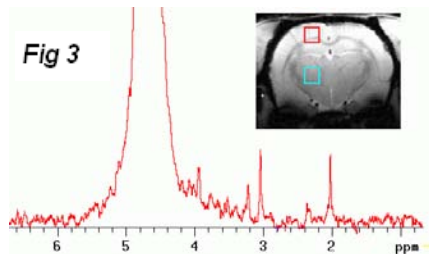
Analysis of the derived CBF values showed a good correlation with mean arterial blood pressure (MABP) and blood PaCO<sub>2</sub>, both of which are important perfusion indexes. A linear multi-regression analysis on all rats in Group 1 gave the following expression ( $R^2=0.96$ ):  $\text{CBF} = \text{CBF}_0 + A \cdot (\text{MABP} - 100) + B \cdot (\text{PaCO}_2 - 40)$ , where  $\text{CBF}_0 = 1.01 \pm 0.31 \text{ ml} \cdot \text{g}^{-1} \cdot \text{min}^{-1}$ ,  $A = 0.0216 \pm 0.0038 \text{ ml} \cdot \text{g}^{-1} \cdot \text{min}^{-1} \cdot \text{mmHg}^{-1}$ , and  $B = 0.0136 \pm 0.0068 \text{ ml} \cdot \text{g}^{-1} \cdot \text{min}^{-1} \cdot \text{mmHg}^{-1}$ . The quality of the correlation is demonstrated in Fig. 2 (filled squares). The CBF values directly measured via the microsphere tracer technique are plotted



in the same graph for comparison (Fig 2, open circles). Abscissa is CBF calculated from regression expression with MABP and PaCO<sub>2</sub> values as inputs. Ordinate is CBF obtained either from the theoretical modeling of measured brain temperature distribution (Group 1, filled squares) or from microsphere direct measurement of CBF (Group 2, open circles). The two independent CBF measurements are in a very good agreement.

An example of spectroscopy data obtained from a single voxel (600 averages) is shown in Fig. 3. The inset represents a high resolution image indicating positions of the most superficial (red square) and the deepest (blue square) voxels. A typical example of brain temperature profile obtained in this way is plotted in Fig. 4 (axes are the same as Fig. 1). Error bars are standard deviation of two FIDs (add-up of first 300 and last 300) in each voxel (5<sup>th</sup> and 6<sup>th</sup> voxels not shown).

Temperature was calculated from previously published



correlation of water-NAA chemical shift difference and absolute brain temperature [3]. The MRS study (Group 3) revealed that in the intact rat brain (under anesthesia, without any surgery and invasive temperature probes), the temperature gradient is much smaller than in the surgically examined rats. The surface region (1mm deep, cortex) temperature is  $0.91 \pm 0.35 \text{ }^\circ\text{C}$  below body temperature, and the deep brain region (4-6mm from surface, thalamus) is  $0.28 \pm 0.11 \text{ }^\circ\text{C}$  below body temperature (inter-animal averages).

**Conclusion** This study using a microsphere tracer technique confirms the theoretically predicted dependence of brain temperature distribution on CBF. The brain temperature profiles were measured independently by MR spectroscopy and directly by thermocouples. These findings emphasize that CBF has marked influence on cortical brain temperature and may substantially affect brain function, including response to functional activation.

**References** [1] Zhu M, et al., J Therm Biol 2004;29(7-8):599. [2] Sukstanskii AL and Yablonskiy DA., J Therm Biol 2004;29(7-8):583. [3] Zhu M, et al., ISMRM 2005;551. [4] Garwood M and Delabarre L., J Magn Reson 2001;153(2):155. [5] Gruetter R, Magn Reson Med 1993;29(6):804.

**Acknowledgements** This study was supported by NIH Grants RO1-NS41519; R24-CA83060 (Small Animal Imaging Resource Program)